This paper was published in the proceedings of
Emerging Lithographic Technologies, SPIE Vol. 3048, pp. 76-88.

Three-Dimensional Electron Beam Lithography Simulation

Chris A. Mack
FINLE Technologies, Austin, TX

Abstract

A new model called ProBEAM/3D is introduced for the simulation of electron beam lithography. Monte Carlo simulations are combined with a beam shape to generate a single “pixel” energy distribution. This pixel is then used to write a pattern by controlling the dose of every pixel on an address grid. The resulting dose pattern is used to expose and develop a resist to form a three-dimensional resist pattern.

I. Introduction

Electron beam lithography continues to play a vital role in semiconductor and nanotechnology. Current and future demands on the mask making process require tight control over every aspect of the electron beam lithography process. In addition, direct write raster and shaped beam lithographies continue to look promising for research and possibly future manufacturing. As a result, the need to understand and optimize electron beam lithography is greater than ever.

Lithography modeling has proven an invaluable tool in the use and development of optical lithography over the years. Although electron beam simulation has also been used extensively, it has not undergone the level of development seen in optical lithography simulation. In particular, resist exposure and development models for electron beam lithography are relatively crude compared to the equivalent models for optical resists. In addition, one of the unique capabilities of electron beam lithography, its flexibility in writing strategies, remains difficult to apply using simulation.

This paper will present a new model for three-dimensional electron beam lithography simulation called ProBEAM/3D. Beginning with standard Monte Carlo techniques to calculate the “point spread” electron energy distribution, any beam shape can be used to create the energy distribution due to a “spot” exposure. A flexible writing strategy definition will be presented to allow easy simulation of many possible writing strategies. Well known models of resist exposure and development chemistry will be applied. Both conventional and chemically amplified resists can be simulated. The combination of the individual parts will yield a comprehensive model able to predict three-dimensional resist profiles for a wide range of electron beam lithography tools and resist processes.

II. Structure of the Model

The overall electron beam simulation package is structured into a set a modular components, the purpose of which is to promote the reuse of simulation results. The first module, the Monte Carlo calculations, predicts the interaction of an electron of a given energy with a given resist/substrate film stack. The result is independent of the details of the actual electron beam spot size and the pattern to be written. Thus, the output of the Monte Carlo module can be saved and reused whenever the beam energy and film stack are the same. A library of common energies and film stacks can be built up over time.

The second module, called Pixel Generation, takes the output of the Monte Carlo module and combines it with the details of the electron beam spot shape to create a “spot” or “pixel” image in the resist. The result is the energy distribution within the resist for a given electron beam (Gaussian or shaped) of a given beam energy and for a given film stack. Again, a library of pixels for common beam geometries, energies, and film stacks can be built up and stored for later reuse.

Once a pixel image in the resist has been calculated, this pixel can be used to write a pattern in the resist. A “mask” pattern is overlaid with an address grid to specify the dose for each pixel. The result is a three-dimensional image of deposited energy within the resist. This image then exposes the resist material, which can be positive or negative acting, conventional or chemically amplified. A post-exposure bake can be used to diffuse (and possibly react) chemical species in the exposed resist, followed by a three-dimensional development to give the final resist profile. The general sequence of events is pictured in Figure 1.

The following sections will describe each step in the modeling sequence in more detail.

III. Monte Carlo Calculations

The Monte Carlo calculations use standard techniques that have been extensively reported in the literature [1-9]. In particular, the method of Hawryluk, Hawryluk, and Smith [7] is followed. An electron scatters off nuclei in a pseudo-random fashion. The distance between collisions follows Poisson statistics using a mean free path based on the scattering cross-section of the nuclei. The energy loss due to a scattering event is calculated by the Beth energy loss formula. The “continuous slowing-down approximation” is used to spread this energy over the length traveled. Many electrons (typically 50,000 - 100,000) are used to bombard the material and an average energy deposited per electron as a function of position in the solid is determined.

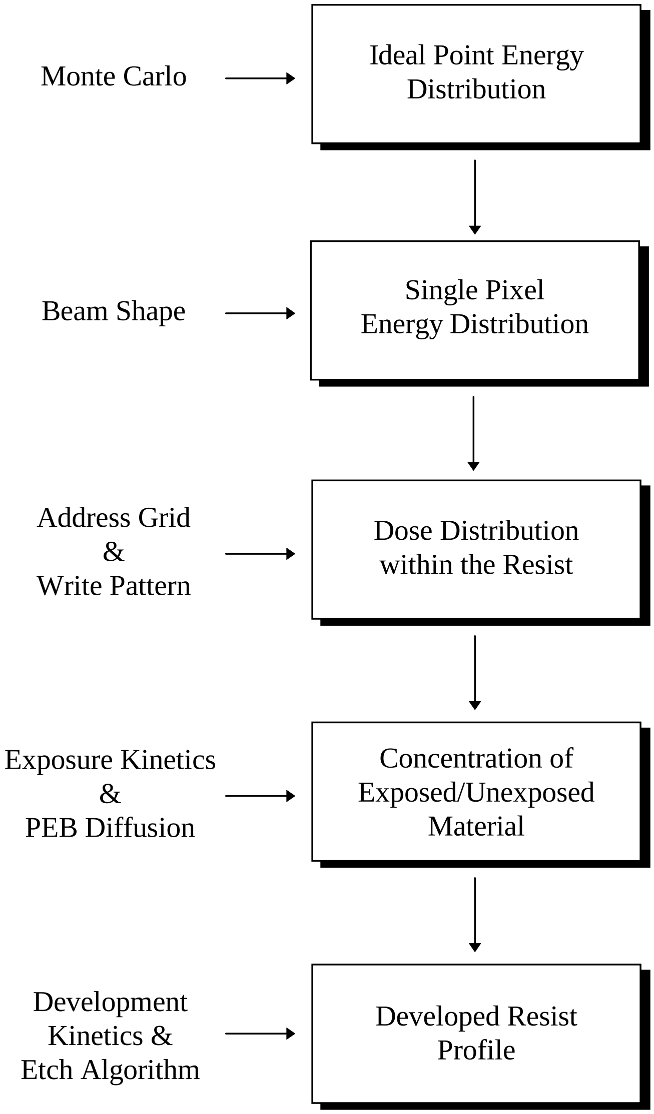

Figure 1. Flow diagram of ProBEAM/3D

Some results of the Monte Carlo calculations are shown in Figures 2-4. For comparison purposes, the simulation conditions were set to match those shown in Ref. 1, pages 106 - 109. Figure 2 shows the electron trajectories of 100 25KeV electrons in silicon, copper, and gold. The deposited energy distributions resulting from these trajectories are shown in Figure 3 (using 100,000 electrons to get good statistics) where the physically-based assumption of radial symmetry is used to collect deposited energy in radial bins. Finally, Monte Carlo trajectories in resist on silicon are shown in Figure 4 for different beam energies.

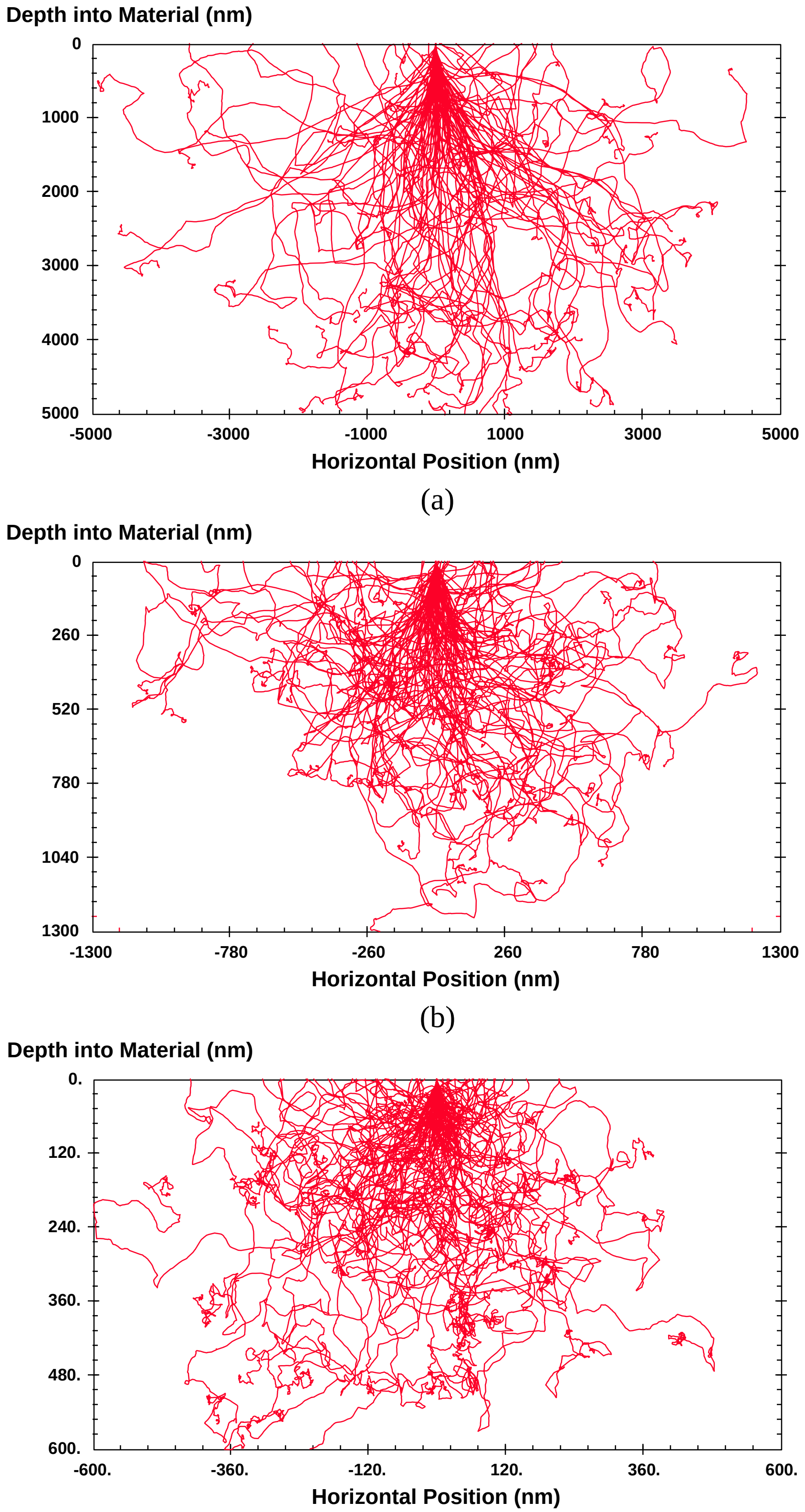

(a)

(b)

(c)

Figure 2. Monte Carlo results for 25KeV incident electrons on (a) silicon, (b) copper, and (c) gold (compare to Ref. 1, page 106).

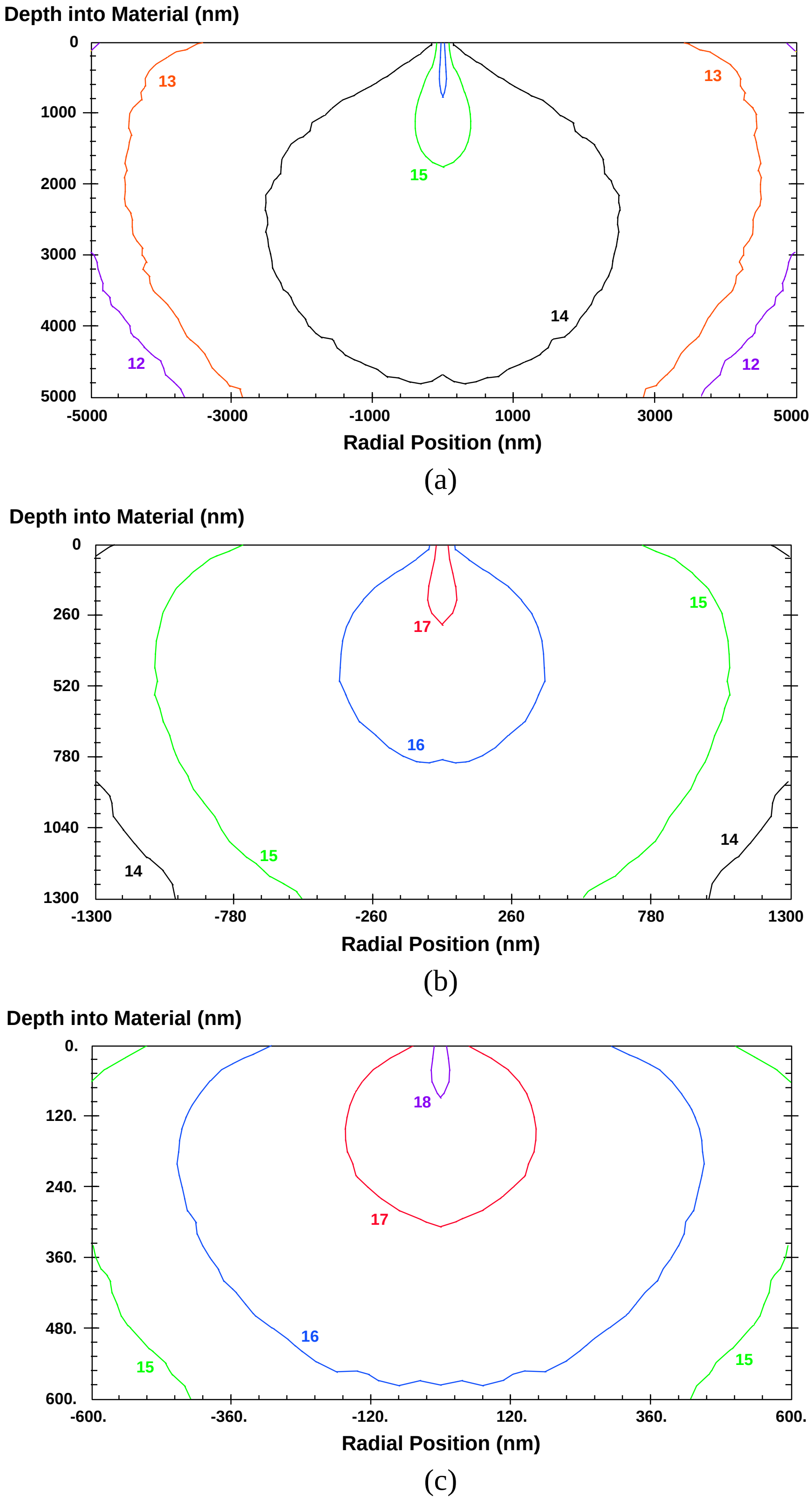

(a)

(b)

(c)

Figure 3. Deposited energy distributions (corresponding to Figure 2) for 25KeV incident electrons on (a) silicon, (b) copper, and (c) gold (compare to Ref. 1, page 108). Contours show $\log_{10}(eV/cm^3/electron)$.

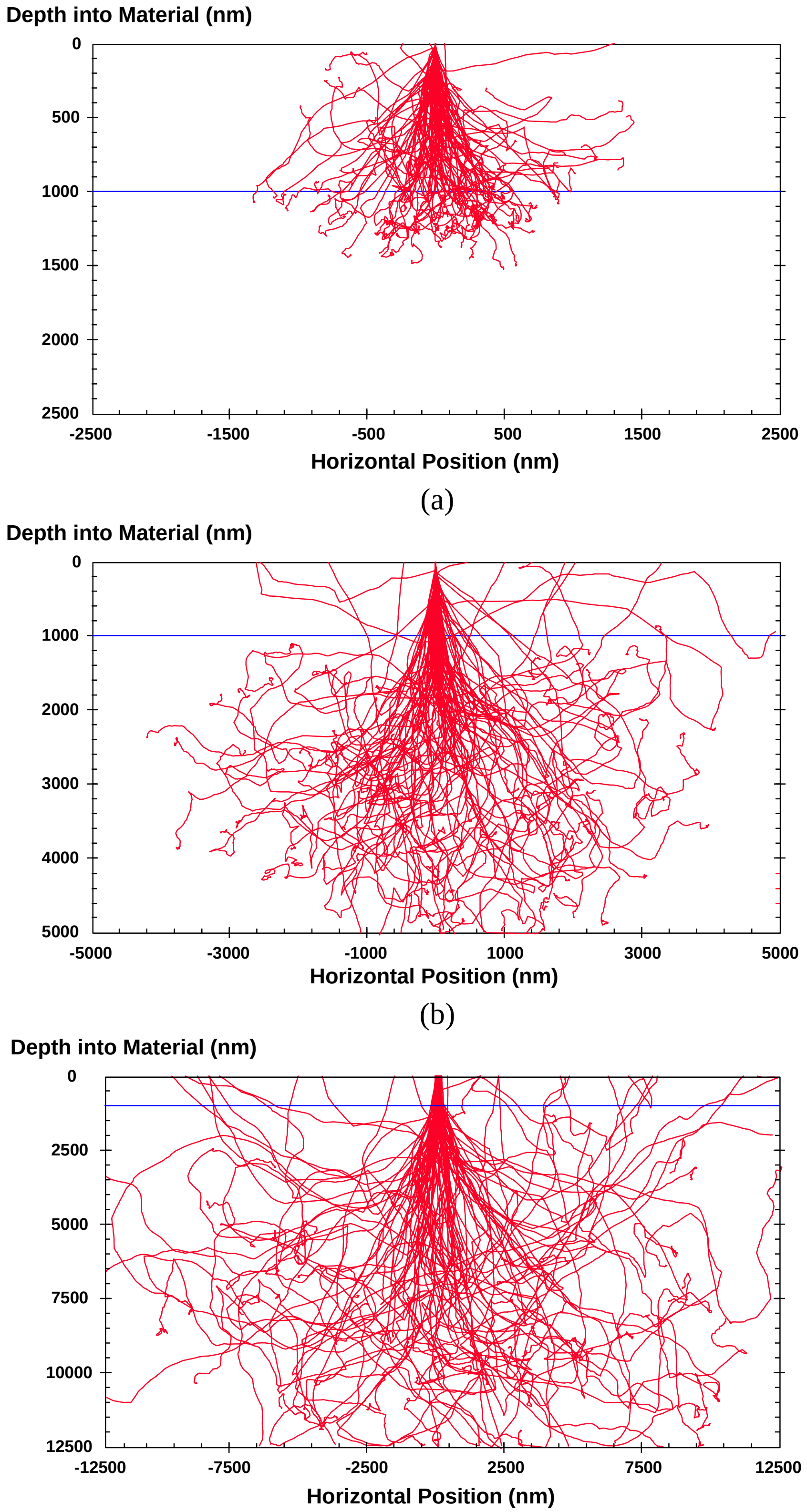

(a)

(b)

(c)

Figure 4. Monte Carlo results for 1μm of PMMA on silicon for (a) 10KeV, (b) 25KeV, and (c) 50KeV electron beam energies.

IV. Pixel Generation

The final result of the Monte Carlo calculation is the average energy distribution of a single electron of a given initial energy normally incident on the material/film stack at a single point. Electron beam exposure tools generate a spot or pixel of many electrons in a certain shape in order to expose the resist. For example, a typical e-beam exposure tool may use an electron beam that can be well approximated by a Gaussian-shaped spot of a certain full width at half maximum (FWHM). The Monte Carlo result can be used to generate a "pixel", the deposited energy for an average electron in the electron beam spot. The pixel is generated as the convolution of the Monte Carlo point energy distribution with the beam shape.

Figure 5 shows two example pixels, one for a Gaussian shaped beam of 250nm FWHM and the second for a uniform square pixel with Gaussian edges (125nm square center with a 125nm FWHM Guassian split between right and left edges).

V. Beam Writing Strategy

The beam writing strategy used in ProBEAM/3D was developed to mimic the behavior of common electron beam lithography tools. A square address grid is defined with any grid size possible. Centered at each grid point is a beam pixel as described in the preceding section. Each pixel address is then assigned a dose (for example, in $\mu C/cm^2$) which essentially determines the number of electrons used in each pixel. The e-beam image is then the sum of the contributions from each pixel. In the simplest scheme, pixels are either turned on or off to provide the desired pattern.

Since each individual pixel can be controlled in dose, this writing strategy is very flexible. Proximity correction schemes and "gray-scale" exposure doses can easily be accommodated.

Figure 6 shows the results of a typical exposure pattern. The write pattern is turned on and off to produce a square 2.4μm contact with 0.8μm serifs on each corner. The 250nm Gaussian pixel of Figure 5b was used on a 200nm address grid. The off pixels were completely off and the on pixels were given a dose of $4\mu C/cm^2$.

VI. Resist Exposure and Development

Resist exposure and development models have been borrowed from optical lithography simulation [10-13] and applied to e-beam lithography. The Dill exposure model [10,11] is based on a first order chemical reaction of some radiation-sensitive species of relative concentration *m*.

$$\frac{dm}{dE} = -Cm \tag{1}$$

where E is the e-beam deposited exposure dose at some point in the resist (in eV/cm^3) and C is the exposure rate constant (with units of 1/dose). The solution to this rate equation is a simple exponential.

$$m = e^{-CE} \tag{2}$$

The relative sensitizer concentration m (or the reaction product of concentration 1-m) then controls the development process. The Mack kinetic model [12] or the enhanced kinetic model [13] can then be applied. The standard Mack model takes the form (for a positive resist)

$$r = r_{\max} \frac{(a+1)(1-m)^n}{a+(1-m)^n} + r_{\min} \tag{3}$$

where r_{max} is the maximum development rate for completely exposed resist, r_{min} is the minimum development rate for completely unexposed resist, n is the dissolution selectivity (proportional to the resist contrast), and a is a simplifying constant given by

$$a = \frac{(n+1)}{(n-1)}\left(1 - m_{TH}\right)^n \tag{4}$$

where m_{TH} is called the threshold value of m. For a negative resist, the terms 1-m in equations (3) and (4) are replaced by m.

Chemically amplified resist can also be simulated using reaction-diffusion models developed for optical lithography [14,15].

Full three-dimensional simulation can be performed by ProBEAM/3D by pulling together all of the components described above. Figure 7 shows the resulting m distributions after exposure for the dose profiles given in Figure 6 assuming an exposure rate constant of 0.005μm^3/mJ. Figure 8 shows the final 3D resist profile after development.

VII. Conclusions

The importance of lithography simulation as a research, development and manufacturing tool continues to grow. Likewise, pressing demands on current and future mask making requirements and the possibility of a greater role for direct-write have made electron beam lithography even more critical. This paper presents a new tool for studying the intricacies of e-beam lithography called ProBEAM/3D. Monte Carlo simulations are combined with a beam shape to generate a single “pixel” energy distribution. This pixel is then used to write a pattern by controlling the dose of every pixel on an address grid. The resulting dose pattern is used to expose and develop a resist to form a three-dimensional resist pattern.

References

1. N. Eib, D. Kyser, and R. Pyle, “Electron Resist Process Modeling,” Chapter 4, Lithography for VLSI, VLSI Electronics - Microstructure Science Volume 16, R. K. Watts and N. G. Einspruch, eds., Academic Press (New York:1987) pp. 103-145.
2. Electron-Beam Technology in Microelectronic Fabrication, George R. Brewer, ed., Academic Press (New York:1980).
3. Kamil A. Valiev, The Physics of Submicron Lithography, Plenum Press (New York:1992).
4. L. A. Kulchitsky and G. D. Latyshev, “The Multiple Scattering of Fast Electrons,” *Physical Review*, Vol. 61 (March 1, 1942) pp. 254-265.
5. K. Murata, T. Matsukawa, and R. Shimizu, “Monte Carlo Calculations on Electron Scattering in a Solid Target,” *Japanese Journal of Applied Physics*, Vol. 10, No. 6 (June, 1971) pp. 678-686.
6. R. Shimizu and T. E. Everhart, “Monte Carlo Simulation of the Energy Dissipation of an Electron Beam in an Organic Specimen,” *Optik*, Vol. 36, No. 1 (1972) pp. 59-65.
7. R. J. Hawryluk, A. M. Hawryluk, and H. I. Smith, “Energy Dissipation in a Thin Polymer Film by Electron Beam Scattering,” *Journal of Applied Physics*, Vol. 45, No. 6 (June, 1974) pp. 2551-2566.
8. D. F. Kyser and N. S. Viswanathan, “Monte Carlo Simulation of Spatially Distributed Beams in Electron-Beam Lithography,” *Journal of Vacuum Science and Technology*, Vol. 12, No. 6 (Nov/Dec, 1975) pp. 1305-1308.
9. M. G. Rosenfield, A. R. Neureuther, and C. H. Ting, *Journal of Vacuum Science and Technology*, Vol. 19, No. 4 (Nov/Dec, 1981) pp. 1242-.
10. F. H. Dill, W. P. Hornberger, P. S. Hauge, and J. M. Shaw, “Characterization of Positive Photoresist,” *IEEE Trans. Electron Dev.*, ED-22, No. 7, (1975) pp. 445-452, and *Kodak Microelec. Sem. Interface '74* (1974) pp. 44-54.
11. C. A. Mack, “Absorption and Exposure in Positive Photoresist,” *Applied Optics*, Vol. 27, No. 23 (1 Dec. 1988) pp. 4913-4919.
12. C. A. Mack, “Development of Positive Photoresist,” *Jour. Electrochemical Society*, Vol. 134, No. 1 (Jan. 1987) pp. 148-152.
13. C. A. Mack, “New Kinetic Model for Resist Dissolution,” *Jour. Electrochemical Society*, Vol. 139, No. 4 (Apr. 1992) pp. L35-L37.
14. C. A. Mack, “Lithographic Effects of Acid Diffusion in Chemically Amplified Resists,” *OCG Microlithography Seminar Interface ‘95, Proc.*, (1995) pp. 217-228, and Microelectronics Technology: Polymers for Advanced Imaging and Packaging, ACS Symposium Series 614, E. Reichmanis, C. Ober, S. MacDonald, T. Iwayanagi, and T. Nishikubo, eds., ACS Press (Washington: 1995) pp. 56-68.
15. J. S. Petersen, C. A. Mack, J. Sturtevant, J. D. Myers and D. A. Miller, “Non-constant Diffusion Coefficients: Short Description of Modeling and Comparison to Experimental Results,” *Advances in Resist Technology and Processing XII, Proc.*, SPIE Vol. 2438 (1995) pp. 167-180.

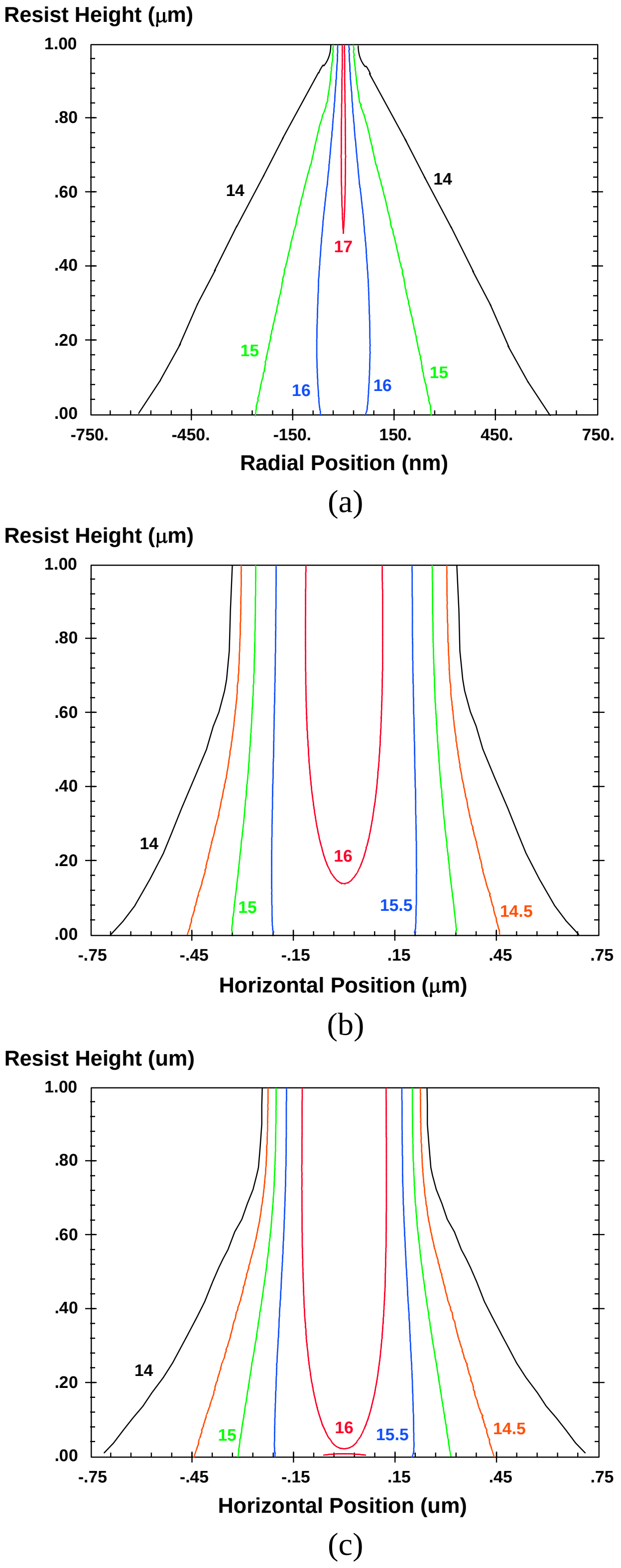

Figure 5. Monte Carlo and pixel generation results for 1μm of PMMA on silicon with 25KeV electrons: (a) Monte Carlo "point" energy distribution, (b) pixel result for a 250nm (FWHM) Gaussian beam, and (c) pixel result for a 125nm square beam with 125nm Gaussian edges. Contours show $\log_{10}(\text{eV/cm}^3\text{/electron})$.

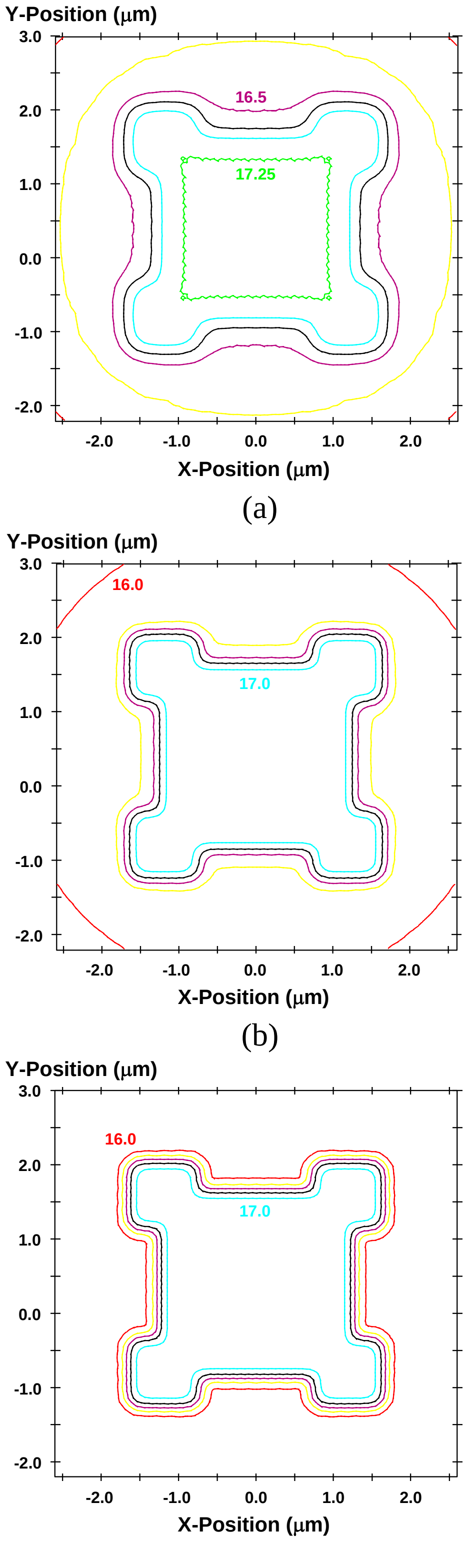

(a)

(b)

(c)

Figure 6. Dose distributions in 1μm of PMMA on silicon with 25KeV electrons for a dose of 4μC/cm^2 at (a) top of the resist, (b) middle of the resist, and (c) bottom of the resist. Contours show $\log_{10}$(eV/cm^3).

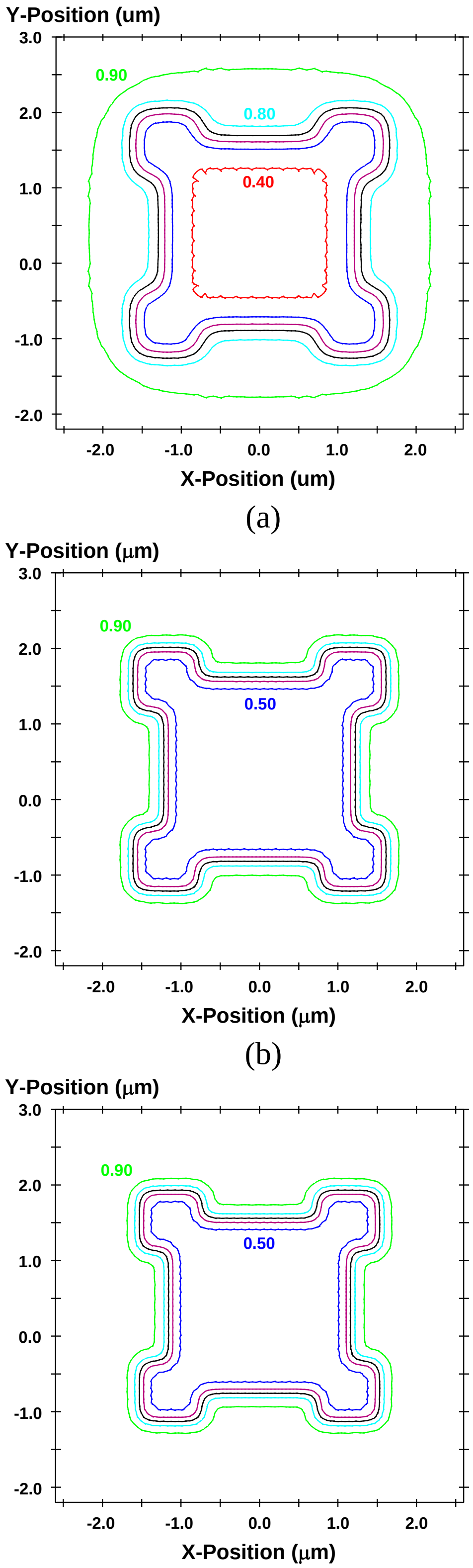

(a)

(b)

(c)

Figure 7. Relative concentration of e-beam sensitive material as a result of exposure based on Figure 6 at (a) top of the resist, (b) middle of the resist, and (c) bottom of the resist.

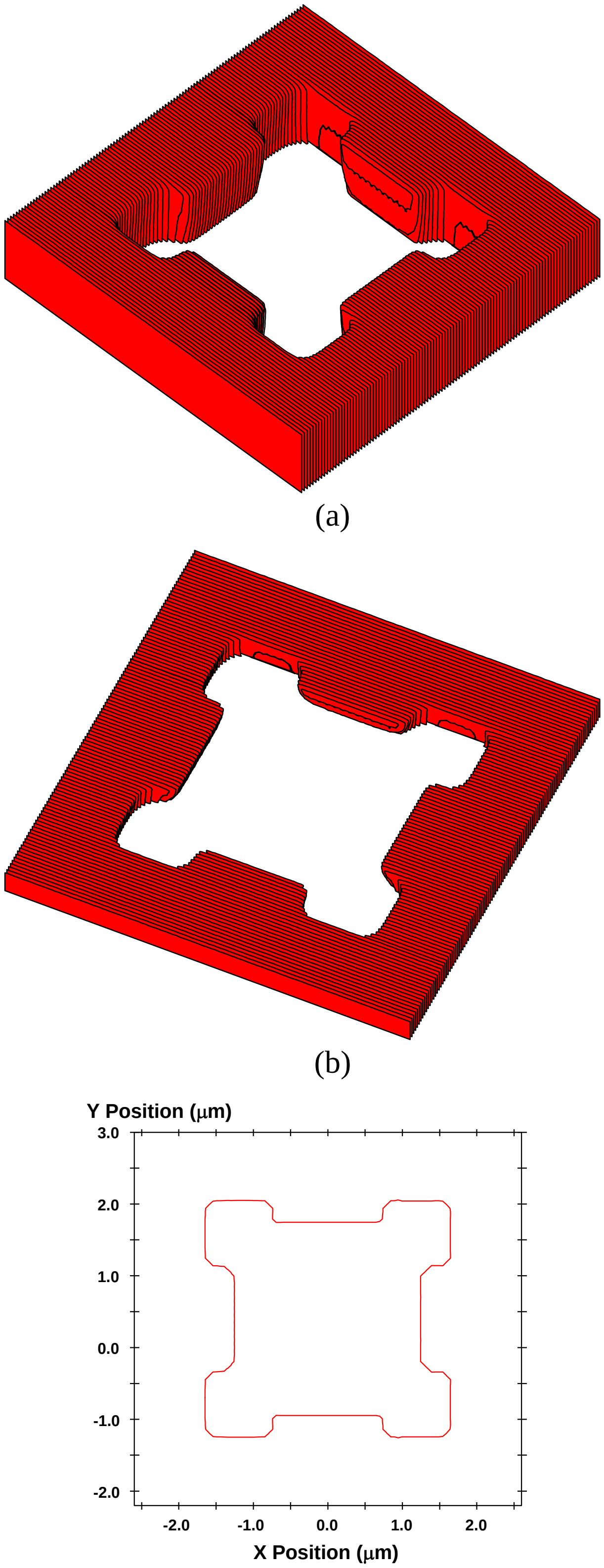

(a)

(b)

(c)

Figure 8. Three-dimensional resist profile at different viewing angles (a&b), as well as a top-down view (c).